



Chitosan-based nanofibrous membranes for antibacterial filter applications

Ashleigh Cooper^a, Rachael Oldinski^b, Hongyan Ma^b, James D. Bryers^b, Miqin Zhang^{a,*}

^a Department of Materials Science & Engineering, University of Washington, Seattle, WA 98195, USA

^b Department of Bioengineering, University of Washington, Seattle, WA 98195, USA

ARTICLE INFO

Article history:

Received 9 August 2012

Received in revised form 27 August 2012

Accepted 31 August 2012

Available online 7 September 2012

Keywords:

Microfiltration

Nanofiber

Chitosan

Antibacterial

Water permeability

ABSTRACT

Nanofibrous membranes have drawn considerable interest for filtration applications due to their ability to withstand high fluid flux while removing micro- and nano-sized particulates from solution. The desire to introduce an antibacterial function into water filter applications presents a challenge to widespread application of fibrous membranes because the addition of chemicals or biocides may produce harmful byproducts downstream. Here, we report the development of chitosan–polycaprolactone (PCL) nanofibrous membranes to utilize the natural antibacterial property of chitosan for antibacterial water filtration. Chitosan–PCL fibers with diameters of 200–400 nm and chitosan contents of 25, 50 and 75 wt% were prepared by electrospinning. In a series of bacterial challenge tests, chitosan–PCL fibrous membranes significantly reduced *Staphylococcus aureus* adhesion compared to PCL fibrous membranes. In water permeability and particulate size removal tests, fibrous membranes with 25% chitosan supported the greatest water flux ($\sim 7000 \text{ L/h/m}^2$) with 100% removal of 300-nm particulates, while maintaining the membrane integrity. This study demonstrates the potential of chitosan–PCL nanofibrous membranes as pre-filters for water filtration systems that demonstrate combinatorial filtration and intrinsic antibacterial advantages.

© 2012 Elsevier Ltd. All rights reserved.

1. Introduction

More than 1 billion people worldwide lack access to affordable, potable water resulting in increased health risks associated with waterborne illnesses (Nations, 2003). Methods currently used to purify water of pathogens and bacteria rely on direct chemical treatments, which can potentially produce harmful byproducts downstream (Gomez et al., 2006). Consequently, filtration has emerged as a cost effective and chemical-free approach for the decontamination and purification of water supplies (Li & Chase, 2010; Porcelli & Judd, 2010; Sato, Wang, Ma, Hsiao, & Chu, 2011). Nanofibrous membranes have increased porosity and an interconnected pore structure that results in increased permeability and thus high-throughput compared to membranes of microfibers. Nanofibrous membranes with pore sizes of $0.45 \mu\text{m}$ selectively remove bacteria (Gomez et al., 2006), as the bacterium size, i.e. $1.6 \times 0.8 \mu\text{m}$ for *Pseudomonas aeruginosa*, $2 \times 1 \mu\text{m}$ for *Escherichia coli* and $0.8 \mu\text{m}$ for *Staphylococcus aureus*, are larger than the membrane pore size (Lebleu, Roques, Aimar, & Causserand, 2009). In combination with nanofibrous membranes, antibacterial agents are often used to kill or inhibit

the growth of bacteria that would otherwise lead to biofouling and decreased filter efficiencies (Botes & Eugene Cloete, 2010). Nanofibrous membranes with an exogenic antibacterial agent, such as polyamide/poly(dimethylimino)(2-hydroxy-1,3-propanedilyl)chloride (Daels et al., 2011), cellulose acetate/silver nanoparticles (Lala et al., 2007), poly(vinylidene fluoride)/silver nanoparticles (Yuan et al., 2009), chitosan/polyvinyl alcohol/silver nitrate/TiO₂ (Son, Yeom, Song, Lee, & Hwang, 2009), and inorganic silica/silver nanoparticles (Kyung, Kwark, & Park, 2007) have been developed to release their biocidal agents during filtration. In this study, we report the development of a chitosan-based nanofibrous membrane with inherent antibacterial properties to improve safety and efficacy of filtration.

Chitosan exhibits antimicrobial properties towards bacteria, viruses, and fungi, for which many strains have been assayed (Muzzarelli et al., 1990, 2001; Rabea, Badawy, Stevens, Smagghe, & Steurbaut, 2003). The antimicrobial mechanism includes the initial deposition of a chitosan coat on the anionic cell wall, with subsequent alteration of biochemical functions, and damage to internal organelles by internalized chitosan oligomers (Kong, Chen, Xing, & Park, 2010; Liu, Du, Wang, & Sun, 2004; Muzzarelli et al., 1990). Chitosan (in the solid-state as well) exhibits a cationic surface charge at physiological pH values (Hoven, Tangpasuthadol, Angkitpaiboon, Vallapa, & Kiatkamjornwong, 2007; Matienzo & Winnacker, 2002; Matsumoto, Yako, Minagawa, & Tanioka, 2007), but only a few studies have investigated it as a component in antimicrobial filters. Desai et al., illustrated bacteriostatic reduction

* Corresponding author at: 302L Roberts Hall, Department of Materials Science and Engineering, University of Washington, Seattle, WA 98195, USA.
Tel.: +1 206 616 9356; fax: +1 206 543 3100.

E-mail address: mzhang@u.washington.edu (M. Zhang).

Table 1

Solution concentrations used for electrospinning to produce different fiber compositions.

Solution concentrations used (wt%)		
Fiber compositions	Chitosan	PCL
100% PCL		10%
25% chitosan, 75% PCL	7%	12%
50% chitosan, 50% PCL	7%	12%
75% chitosan, 25% PCL	5%	12%

on chitosan–polyethylene oxide fibers at pH 7.08, however the fiber membranes lacked structural integrity under a filter pressure of 2 mm Hg ($\sim 2 \times 10^{-3}$ bar, 0.2 kPa), resulting in large tears in the membrane (Desai et al., 2009). It is therefore of interest to develop an antibacterial, solid-state chitosan-based nanofibrous filter that can sustain filtration pressures, exhibit high permeability, selectively remove particles based on size and provide a safe antibacterial mode of action for water filtration applications.

Polycaprolactone (PCL) is commonly found in tissue engineering applications due to its structural and mechanical stability (Gross & Kalra, 2002; Hollister, 2005). We have previously reported the design and electrospinning fabrication of non-woven nanofibrous membranes comprised of chitosan and PCL with good mechanical and biological properties favorable for tissue regeneration (Cooper, Jana, Bhattacharai, & Zhang, 2010). In this study, chitosan–PCL fibrous membranes were prepared with different amounts of chitosan to impart an antibacterial property to the membrane. These fibers were prepared without chemical crosslinking or harmful biocides to demonstrate the intrinsic antibacterial characteristics of chitosan for filtration application. The morphology, mechanical properties, and permeability of the membranes were characterized with scanning electron microscopy (SEM), transmission electron microscopy (TEM), tensile testing, water flow permeability tests and particulate removal tests. A bacterial challenge with *S. aureus*, a Gram-positive bacterium, was performed to evaluate the antibacterial performance of the membranes.

2. Materials and methods

2.1. Electrospinning solution preparation

Chitosan and PCL solutions were prepared separately, and then mixed to create a solution of chitosan–PCL. Chitosan (85% deacetylated, Aldrich, St. Louis, MO) was dissolved in 7 wt% trifluoroacetic acid (TFA, Aldrich) and refluxed at 70 °C for 3 h, and PCL was dissolved in 2,2,2-trifluoroethanol (TFE, Aldrich). In preparation of the electrospinning solutions with different polymer concentrations, chitosan (5 and 7 wt%) and PCL (10 and 12 wt%) solutions were prepared. Chitosan–PCL electrospinning solutions were prepared according to Table 1. Immediately prior to electrospinning, the chitosan and PCL solutions were mixed to produce a chitosan–PCL solution with the desired final polymer ratio. A 10% PCL solution in TFE was prepared as a PCL electrospinning solution.

2.2. Electrospinning and characterization of fibrous mats

To produce electrospun nanofibers, approximately 2 mL of the solution was placed in a 3 mL syringe. The syringe tip was placed approximately 20 cm from a fiber collector, oriented -25° from the horizontal, and a 22 kV voltage supply was used to charge the solution. The solution was discharged towards a rotating grounded drum (200 rpm) to collect randomly oriented fibrous mats, with individual fibrous mats being $\sim 100 \mu\text{m}$ in thickness. The collected mats were allowed to dry overnight under a chemical hood and then were attached to a coverslip using biocompatible

poly-L-lactide (Boehringer Ingelheim, Germany) dissolved in hexafluoroisopropanol (Aldrich) at 3.5 wt%. Chitosan–PCL non-porous films (as a two-dimensional control) were prepared by spin-coating the dilute chitosan–PCL solution onto a coverslip. All the fibers and films were neutralized with 14% ammonium hydroxide for 5 min to remove residual acid, followed by rinsing three times with DI water for 5 min each. SEM and TEM were used for morphological and phase analysis. For SEM, the samples were coated with gold for 30 s with 18 mA current applied to a Pt target. The samples were imaged with a JEOL 7000F SEM (JEOL Ltd., Japan) at an accelerating voltage of 5–10 kV. For TEM analysis, samples were transferred to a PELCO folding copper grid and imaged with a Philips CM100 transmission electron microscope.

2.3. Static bacterial challenge

For the bacterial challenge experiments, the samples were disinfected with 70% ethanol prior to bacteria seeding. To evaluate bacterial adhesion and biofilm formation on these fibrous samples, *S. aureus* (ATCC 25693) were incubated with fiber-coated glass coverslips in 24-well tissue culture plates. *S. aureus* were streaked on agar plates supplemented with 10 g/L trypticase soy broth (TSB, pH 7.2) and incubated at 37 °C until growing colonies reached desired sizes. For suspended culture inocula, a single colony sample from the streak plate was collected with a sterile loop, added to 25 mL of 10 g/L TSB, and incubated at 37 °C overnight. Bacterial cells from the overnight culture were diluted with 10 g/L fresh TSB to a final concentration of 5×10^4 cells/mL, and then seeded into individual wells of 24-well plates containing fibers and control films ($n=3$). The plates were incubated at 37 °C under rotation at 125 rpm. At each preset time point (8 and 24 h of incubation), samples were removed and washed twice with PBS and placed in a new 10 mL tube with 1.5 mL PBS. Each sample was sonicated for 5 s three times using a needle ultrasonicator. The solution was then serially diluted and placed on TSB plates and the colony forming units (CFU) counted after 8 and 24 h (Tomasiewicz, 1980). Data were represented as CFU per area (colony number on plate \times dilution factor \times 1.5 mL total volume)/(0.01 mL sample volume \times gross surface area of the glass cover plate 0.785 cm^2). After 24 h of bacterial culture, the membranes were fixed for SEM analysis in 3% glutaraldehyde and dehydrated in an ethanol wash series. The membranes were sputter coated with 7 nm of gold prior to SEM imaging.

2.4. Flow cell apparatus and particulate testing

Square membranes of $\sim 2 \text{ cm}$ in width were cut from the nanofibers mats. These square sample membranes were used for individual water flux testing and particulate–water separation testing with an open-ended filtration setup. The fibrous membrane was sandwiched between two plastic plates with $\sim 1 \text{ cm}$ inner diameter holes. The membrane surface was placed horizontally and two tubes ($\sim 1 \text{ cm}$ inner diameter) were coaxially connected to the holes of the top and bottom plastic plates, respectively, to act as an inlet and outlet for water flow. To create a desired pressure on the membrane surface, the inlet was filled with water to a known head height with respect to the membrane surface. To maintain a constant pressure, water was continuously added to keep the head height constant at the inlet. To test the flow rate through the membranes, an inlet pressure between ~ 0.75 and 3 kPa was applied, and the amount of water that passed through the membrane was measured in 1 min increments over a 5-min period.

To test the performance of the membranes for particle separation, polystyrene (PS) particles with 100, 300 and 1000 nm diameters (Sigma–Aldrich) were used. Individual solutions of the PS beads were prepared at 200 ppm in DI water and were allowed to pass through the membranes. To characterize the removal

Table 2

Colony forming units (CFUs, cell number/cm²) of adhered *S. aureus* cells on nanofibrous membranes with different chitosan concentrations.

Cell number/cm ²		
Fiber compositions	8 h	24 h
100% PCL	4.64 ± 1.20	6.45 ± 2.14
25% chitosan	2.02 ± 0.60 ^a	3.79 ± 0.84
50% chitosan	2.54 ± 0.30 ^a	3.61 ± 0.28 ^a
75% chitosan	2.59 ± 0.9	2.92 ± 0.48 ^a

^a Indicates significant difference to 100% PCL fiber.

efficiency of the membranes, the first 2 mL of eluent that passed through the membranes at an initial pressure of ~1.5 kPa were collected. The recovered solution was characterized with a UV–vis spectrometer operated at 490 nm and the concentration of PS nanoparticles was determined from a calibration curve of known PS/DI water concentrations. The membranes were washed briefly with water to remove excess PS beads and prepared for SEM analysis by drying at 37 °C.

2.5. Statistical analysis

Results for bacterial analysis were presented as means ± standard deviation. Statistical analysis was performed using one-way analysis of variance, followed by post hoc Student's *t*-test. Differences were considered significant for values of *p* < 0.05.

3. Results and discussion

Non-woven, randomly oriented fibrous chitosan–PCL membranes were prepared by electrospinning chitosan–PCL solutions containing 0, 25, 50 and 75 wt% of chitosan using a rotating drum setup. The volume of the chitosan–PCL solutions used for preparing an electrospun membrane were the same for all of the ratios (~2 mL) and the electrospinning conditions were controlled to produce similar density membranes composed of nanofibers with approximately the same diameter. As shown in the SEM images of Fig. 1a–d, uniform nanofibrous membranes were formed from all PCL and chitosan–PCL solutions with fiber diameters of 200–400 nm. Pure PCL fibers were electrospun from a 10 wt% PCL/TFE solution (Fig. 1a). Chitosan–PCL fibers with 25 wt% chitosan (Fig. 1b), 50 wt% chitosan (Fig. 1c) and 75 wt% chitosan (Fig. 1d) were electrospun from mixtures prepared from 7 and 12 wt%, 7 and 12 wt%, and 5 and 12 wt% chitosan and PCL solutions, respectively. TEM analysis (Fig. 1e–h) indicated the homogeneity of the solid fibers, with no sign of phase separation or structural voids.

All the prepared membranes were then assessed as an antibacterial surface with *S. aureus* (SA 25693) as a model bacterium to examine the inhibitory effect of increasing chitosan content in the chitosan–PCL membranes. The membranes were incubated with *S. aureus* over the course of a 24-h period. Bacterial cell attachment was quantified by counting the colony-forming units and by SEM imaging. As shown in Table 2, compared to the synthetic PCL fiber control, the chitosan–PCL samples induced less *S. aureus* colonization. At the 24-h time point, the number of attached *S. aureus* cells increased compared to the 8-h time point except for the 75 wt% chitosan membranes, which exhibited no increase from 8 to 24 h. PCL control membranes exhibited the largest increase in adherent bacterial numbers. At 8 h, all chitosan-containing membranes exhibited approximately half of the adherent cell counts versus the PCL control. The cell adhesion increases for the PCL membrane from 8 to 24 h while increases in adherent cell concentration from 8 to 24 h for chitosan-containing membrane were approximately the same for all four membranes. A previous study of chitosan–PCL films cultured with a gram-positive

Table 3

Flux of PCL and chitosan–PCL membranes at a water pressure of 1.5 kPa.

Nanofibrous membrane	Flux (L/h/m ²)
PCL	2756.8 ± 68.9
25% chitosan	6926.8 ± 1143.6
50% chitosan	2629.46 ± 97.3
75% chitosan	N/A

bacterium, *Streptococcus mutans*, demonstrated similar results that with increasing chitosan content (i.e. cationic nature) the bacteria growth is reduced but not completely eliminated (Sarasam, Krishnaswamy, & Madihally, 2006). Although the study by Sarasam et al. demonstrated that the chitosan-based films are not bactericidal, a reduced bacterial growth in the culture media was reported, suggesting that those chitosan–PCL polyblends leached a growth inhibitory compound into the liquid phase.

After 24 h of bacterial culture, the membranes were fixed for SEM analysis to examine *S. aureus* cell accumulation. As shown in Fig. 2a and e, a large bacteria population was observed on the PCL fibrous membrane, indicating that the bacteria proliferated into dense colonies. In contrast, *S. aureus* cells appeared sporadically on chitosan–PCL membranes. Increasing chitosan weight content in chitosan–PCL membranes did not significantly decrease bacterial adhesion (Fig. 2b–d and f–h). The SEM analysis qualitatively agrees with the colony counts shown in Table 2. In this study, the density of bacterial challenge was significantly greater than any situation present in natural environmental conditions, suggesting that the reduction observed within the 24-h time period may be translated to a dramatically extended filter lifetime for real-world conditions.

The permeability is particularly important to filtration application as it dictates the amount of fluid that can be processed for a given time and dimension at a defined applied pressure without damaging the mechanical integrity of the filter (Barhate & Ramakrishna, 2007). The advantages of nanofibrous membranes as filters include small pore sizes that reduce particle size exclusion and have a high surface-area to volume ratio, which can result in high flux. In this study, a range of filtration pressures (0.75–3 kPa) was applied to the nanofibrous membranes, which falls within the range of transmembrane pressures for microfiltration membranes (Bjorge et al., 2009). Nanofibrous membranes as filters are typically used in conjunction with other supports such as microfibers (Homaeigohar, Buhr, & Ebert, 2010); however the focus of this study was only on the pre-filter and its standalone properties. The combination of these chitosan–PCL membranes with a mechanical support could increase the ability to withstand greater transmembrane pressures. In this study, the membranes were exposed to transmembrane pressures of 0.75–3 kPa. Fibrous samples with 50% and 75% chitosan ruptured at 3 kPa. As a result, a pressure of 1.5 kPa was chosen for all subsequent tests. A vertical column of water was applied to the membrane surface at a constant pressure of 1.5 kPa and the amount of water that passed through the membrane was measured in 1-min increments over a 5-min period. Table 3 lists the evaluated flux rates for PCL, 25 wt% and 50 wt% chitosan fiber membranes. The 75% chitosan membrane was also subjected to the same flux test; however the membrane ruptured at this pressure, which was likely due to chitosan swelling. Thus, we concluded that the 75% chitosan fibrous membrane was not suitable for filtration application under aqueous conditions. The 25% chitosan fiber membrane allowed for the highest fluid flux of ~7000 L/h/m². After the flux test, the membrane morphology was examined with SEM (Fig. 3). The PCL membrane showed less uniform pore sizes and some pores collapsed corroborating the relatively low flux. The 25% chitosan membrane exhibited uniform pore dispersion. Alternatively, the 50% chitosan showed a compressed structure similar to that of the PCL membrane, which contributed the relatively low flux.

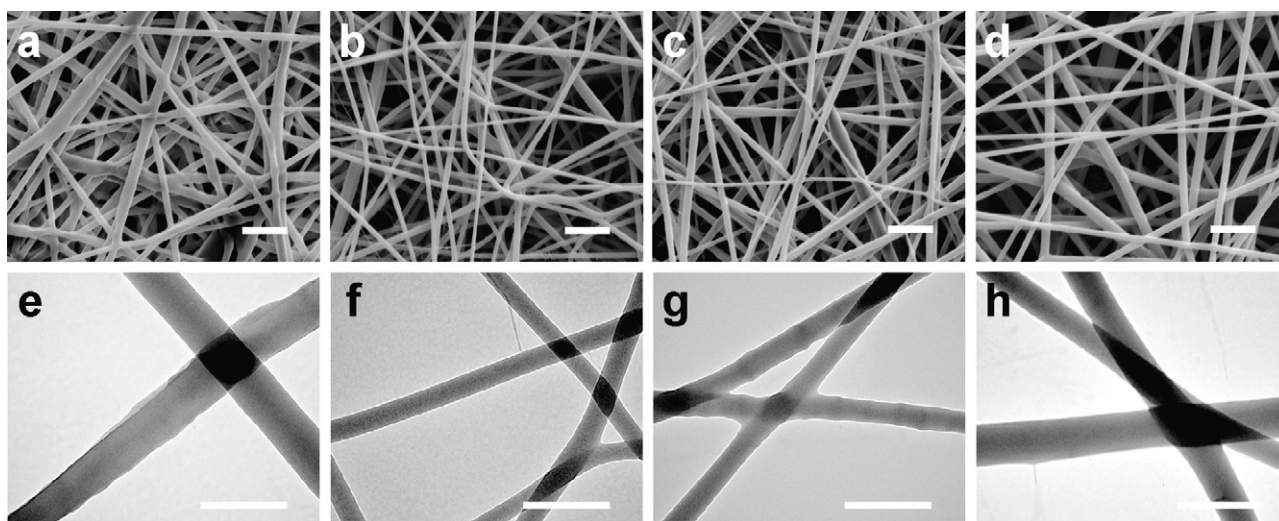


Fig. 1. SEM analysis of nanofibrous membranes with various chitosan concentrations. SEM images of electrospun nanofibrous membranes with (a) PCL only, (b) 25% chitosan and 75% PCL, (c) 50% chitosan and 50% PCL, and (d) 75% chitosan and 25% PCL. The scale bars represent 2 μm in (a–d). TEM images of nanofibrous membranes with (e) PCL only, (f) 25% chitosan, (g) 50% chitosan and (h) 75% chitosan. The scale bars represent 400 nm in (e–h).

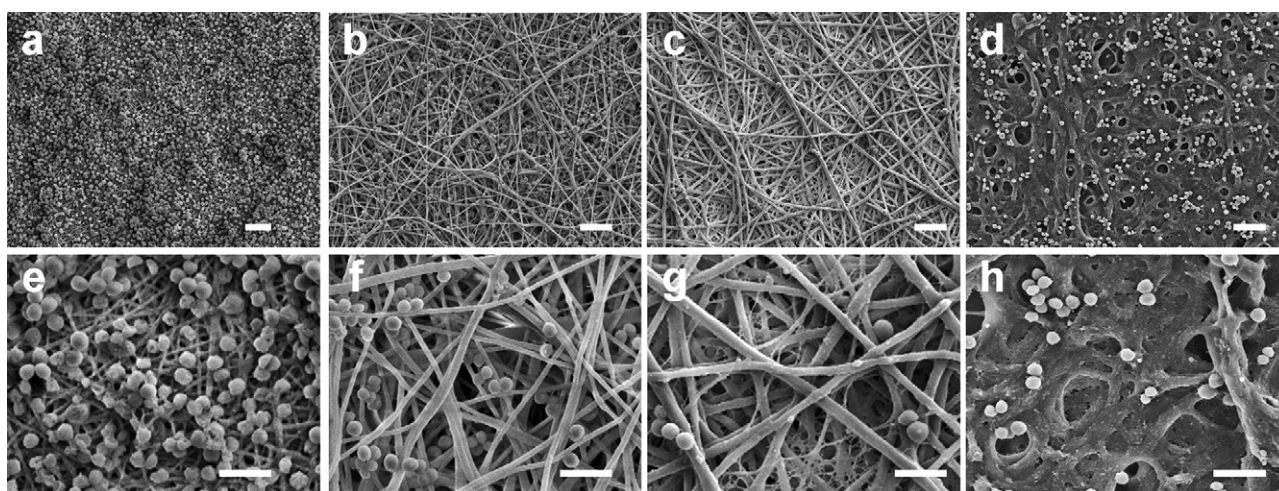


Fig. 2. SEM analysis of *S. aureus* on nanofibrous membranes at low (top row) and high (bottom row) magnifications. (a and e) PCL only, (b and f) 25% chitosan, (c and g) 50% chitosan and (d and h) 75% chitosan. The samples were fixed after 24 h of culture with an initial bacteria density of 5×10^4 cells/mL in tryptic soy broth medium. Scale bars represent 5 μm (top row) and 2.5 μm (bottom row). Note the excessive fiber swelling in h.

Particulate removal, in addition to flux rate, is another primary measure of filter efficacy. To assess the filtering capabilities of the membranes, a series of particulate suspensions comprising polystyrene (PS) beads of different sizes were passed through these membrane filters at a set pressure. The 75 wt% chitosan fiber membrane was not included in this study due to significant material swelling and membrane rupture as mentioned above. Solutions

containing PS beads of 100, 300 and 1000 nm diameters, respectively, were passed through the membranes at 1.5 kPa, and the first 2 mL of eluent was analyzed by UV–vis spectroscopy. The removal efficiency was evaluated by comparing the concentration of the eluent with the concentration of the initial solution (200 ppm). As shown in Table 4, all of the membranes completely removed the large 1000-nm diameter PS beads from the solution (100% removal

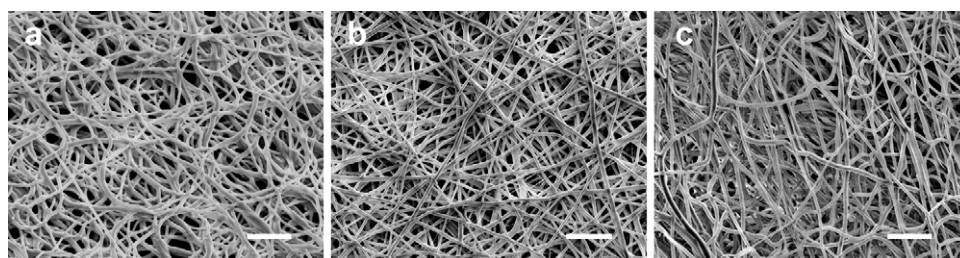


Fig. 3. SEM images of nanofibrous membranes with (a) PCL only, (b) 25% chitosan and (c) 50% chitosan after subjected to water flux for 5 min at 1.5 kPa. The scale bars represent 5 μm .

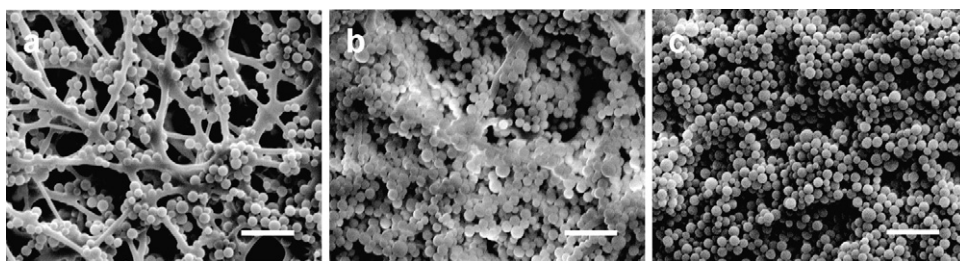


Fig. 4. SEM images of nanofibrous membranes containing (a) PCL only, (b) 25% chitosan and (c) 50% chitosan following a particulate flow study with 300-nm diameter PS beads. The scale bars represent 2 μm .

Table 4
Particulate removal efficiency of membranes with different chitosan concentrations.

Particulate removal efficiency (%)			
Fiber compositions	100 nm	300 nm	1000 nm
50% chitosan	9.25	61.48	100
25% chitosan	14.08	99.76	100
100% PCL	30.63	31.78	100

efficiency). With decreasing bead size, the removal efficiency decreased and varied depending on the membrane material. For 300-nm PS beads, the PCL and 50% chitosan membranes had removal efficiencies of $\sim 31.7\%$ and 61.5% , respectively. Alternatively, the 25% chitosan membrane removed 99.6% of the 300 nm PS beads from the solution. The addition of chitosan to PCL altered the electrospinning behaviors of the solution and effectively reduced the fiber diameters and increased the density. As a result, the addition of PCL created a dense, nanofibrous mat surface that effectively restricted passage of the 300-nm PS particles. The removal efficiency was significantly reduced when the PS beads decreased to 100 nm in size (25%, 15% and 10% for the PCL, 25% and 50% membranes, respectively). Notably, the 25% chitosan–PCL fibrous membrane size-exclusion behavior approached the requirements for HEPA filters (99.7% for 300-nm particulates) (Ahn et al., 2006; Barhate & Ramakrishna, 2007), suggesting the membrane could act as an antibacterial pre-filter for aerosol applications.

SEM was used to analyze the membrane surfaces after 300-nm particulate removal. As shown in Fig. 4a, PS beads adhered strongly to the PCL fibers, wherein the pore size of the membrane was significantly larger than the particle diameter, which could have attributed to its low removal efficiency demonstrated in Fig. 4. Alternatively, the PS beads fully covered the 25% (Fig. 4b) and 50% (Fig. 4c) chitosan membrane surfaces. The resulting beaded surface followed the topography of the fibers, and showed deep penetration into the fiber layers and pores, indicating that the membranes captured the beads, preventing trans-membrane passage. The 25% chitosan–PCL membrane exhibited the best antibacterial behavior, flux performance, and size selectivity down to 300-nm particles. Due to the versatility of the electrospinning method, the porosity, inter-fiber spacing and thickness of a membrane can be controlled to alter the flux and selectivity of a membrane. As a result, the chitosan–PCL membranes can be tailored to specific flux values and particulate removals depending on the application.

4. Conclusions

Nanofibrous membranes were developed via electrospinning with increasing chitosan content to utilize the antibacterial properties of the natural polymer and size-selectivity of the fibrous membranes. We demonstrated that the incorporation of 25% chitosan into the nanofibrous membrane reduced *S. aureus* bacterial colonization by 50% compared to membranes made of pure PCL fibers. With increasing chitosan content, the fibers were more

susceptible to swelling, preventing their application as a filter. At 25 and 50% chitosan content, the highly porous membranes supported high water permeability that did not damage the membrane morphology. Furthermore, a chitosan–PCL fibrous membrane was able to remove near 100% of 300-nm diameter particles, demonstrating the ability to selectively remove particles and act as a pre-filter. The developed membrane combines the antibacterial behavior of natural chitosan polymer with nanofiber advantages to serve as a candidate for microfiltration applications.

Acknowledgements

This work is supported in part by UW TGIF and the Kyocera Professor Endowment. Rachael Oldinsky and James Bryers were supported by the NIH (Grant number: R01DE018701). Ashleigh Cooper would like to acknowledge the support by the Bank of America Endowed Minority fellowships.

References

- Ahn, Y., Park, S., Kim, G., Hwang, Y., Lee, C., Shin, H., et al. (2006). Development of high efficiency nanofilters made of nanofibers. *Current Applied Physics*, 6(6), 1030–1035.
- Barhate, R., & Ramakrishna, S. (2007). Nanofibrous filtering media: Filtration problems and solutions from tiny materials. *Journal of Membrane Science*, 296(1–2), 1–8.
- Bjorge, D., Daels, N., De Vrieze, S., Dejana, P., Van Camp, T., & Audenaert, W. (2009). Performance assessment of electrospun nanofibers for filter applications. *Desalination*, 249(3), 942–948.
- Botes, M., & Eugene Cloete, T. (2010). The potential of nanofibers and nanobiocides in water purification. *Critical Reviews in Microbiology*, 36(1), 68–81.
- Cooper, A., Jana, S., Bhattarai, N., & Zhang, M. (2010). Aligned chitosan-based nanofibers for enhanced myogenesis. *Journal of Materials Chemistry*, 20(1), 8904–8911.
- Daels, N., De Vrieze, S., Samper, I., Decostere, B., Westbroek, P., Dumoulin, A., et al. (2011). Potential of a functionalised nanofibre microfiltration membrane as an antibacterial water filter. *Desalination*, 275(1–3), 285–290.
- Desai, K., Kit, K., Li, J., Michael Davidson, P., Zivanovic, S., & Meyer, H. (2009). Nanofibrous chitosan non-wovens for filtration applications. *Polymer*, 50(15), 3661–3669.
- Gomez, M., De la Rua, A., Garralon, G., Plaza, F., Hontoria, E., & Gomez, M. (2006). Urban wastewater disinfection by filtration technologies. *Desalination*, 190(1–3), 16–28.
- Gross, R. A., & Kalra, B. (2002). Biodegradable polymers for the environment. *Science*, 297(5582), 803–807.
- Hollister, S. J. (2005). Porous scaffold design for tissue engineering. *Nature Materials*, 4(7), 518–524.
- Homaeigohar, S. S., Buhr, K., & Ebert, K. (2010). Polyethersulfone electrospun nanofibrous composite membrane for liquid filtration. *Journal of Membrane Science*, 365(1–2), 68–77.
- Hoven, V. P., Tangpasuthadol, V., Angkitpaiboon, Y., Vallapa, N., & Kiatkamjornwong, S. (2007). Surface-charged chitosan: Preparation and protein adsorption. *Carbohydrate Polymer*, 68(1), 44–53.
- Kong, M., Chen, X. G., Xing, K., & Park, H. J. (2010). Antimicrobial properties of chitosan and mode of action: A state of the art review. *International Journal of Food Microbiology*, 144(1), 51–63.
- Kyung, M. D., Kwark, Y.-J., & Park, W. H. (2007). Preparation of inorganic silica nanofibers containing silver nanoparticles. *Fibers and Polymers*, 8(6), 591–600.
- Lala, N. L., Ramaseshan, R., Bojun, L., Sundarajan, S., Barhate, R., Ying-jun, L., et al. (2007). Fabrication of nanofibers with antimicrobial functionality used as filters: Protection against bacterial contaminants. *Biotechnology and Bioengineering*, 97(6), 1357–1365.

- Lebleu, N., Roques, C., Aïmar, P., & Causserand, C. (2009). Role of the cell-wall structure in the retention of bacteria by microfiltration membranes. *Journal of Membrane Science*, 326(1), 178–185.
- Li, J., & Chase, H. A. (2010). Applications of membrane techniques for purification of natural products. *Biotechnology Letters*, 32(5), 601–608.
- Liu, H., Du, Y., Wang, X., & Sun, L. (2004). Chitosan kills bacteria through cell membrane damage. *International Journal of Food Microbiology*, 95(2), 147–155.
- Matienzo, L. J., & Winnacker, S. K. (2002). Dry processes for surface modification of a biopolymer: Chitosan. *Macromolecular Materials and Engineering*, 287(12), 871–880.
- Matsumoto, H., Yako, H., Minagawa, M., & Tanioka, A. (2007). Characterization of chitosan nanofiber fabric by electrospray deposition: Electrokinetic and adsorption behavior. *Journal of Colloid and Interface Science*, 310(2), 678–681.
- Muzzarelli, R., Muzzarelli, C., Tarsi, R., Millani, M., Gabbanelli, F., & Cartolari, M. (2001). Fungistatic activity of modified chitosans against *Saprolegnia parasitica*. *Biomacromolecules*, 2(1), 165–169.
- Muzzarelli, R., Tarsi, R., Filippini, O., Giovanetti, E., Biagini, G., & Varaldo, P. E. (1990). Antimicrobial properties of N-carboxybutyl chitosan. *Antimicrobial Agents and Chemotherapy*, 34(10), 2019–2023.
- Nations, U. (2003). *Water for people, water for live: The United Nations World Development Report*. UNESCO Publishing/Berghahan Books.
- Porcelli, N., & Judd, S. (2010). Chemical cleaning of potable water membranes: A review. *Separation and Purification Technology*, 71(2), 137–143.
- Rabea, E. I., Badawy, M. E. T., Stevens, C. V., Smagghe, G., & Steurbaut, W. (2003). Chitosan as antimicrobial agent: Applications and mode of action. *Biomacromolecules*, 4(6), 1457–1465.
- Sarasam, A. R., Krishnaswamy, R. K., & Madhally, S. V. (2006). Blending chitosan with polycaprolactone: Effects on physicochemical and antibacterial properties. *Biomacromolecules*, 7(4), 1131–1138.
- Sato, A., Wang, R., Ma, H., Hsiao, B. S., & Chu, B. (2011). Novel nanofibrous scaffolds for water filtration with bacteria and virus removal capability. *Journal of Electron Microscopy*, 60(3), 201.
- Son, B., Yeom, B.-Y., Song, S. H., Lee, C.-S., & Hwang, T. S. (2009). Antibacterial electrospun chitosan/poly(vinyl alcohol) nanofibers containing silver nitrate and titanium dioxide. *Journal of Applied Polymer Science*, 111(6), 2892–2899.
- Tomasiewicz, D. (1980). The most suitable number of colonies on plates for counting. *Journal of Food Protection*, 43(4), 282–286.
- Yuan, J., Geng, J., Xing, Z., Shen, J., Kang, I.-K., & Byun, H. (2009). Electrospinning of antibacterial poly(vinylidene fluoride) nanofibers containing silver nanoparticles. *Journal of Applied Polymer Science*, 116(2), 668–672.